

Why Did the Electron Cross the Road? A Scanning Tunneling Microscopy (STM) Study of Molecular Conductance for the Physical Chemistry Lab

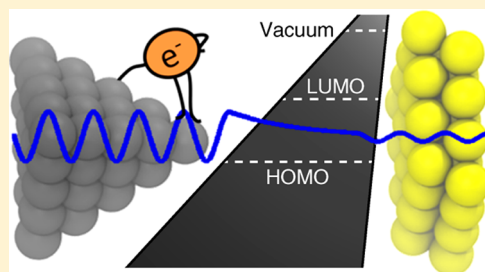
Bradley W. Ewers, Amanda E. Schuckman,[§] and James D. Batteas*

Department of Chemistry, Texas A&M University, College Station, Texas 77842-3012, United States

Supporting Information

ABSTRACT: A series of experiments employing scanning tunneling microscopy (STM) have been developed for the physical chemistry laboratory. These experiments are designed to engage students in cutting edge research techniques while introducing and reinforcing topics in physical chemistry, quantum mechanics, solid-state chemistry, and the electronic structure of molecules and materials. In the first of three experiments, students are introduced to the basics of STM operation while imaging and conducting spectroscopy on the highly oriented pyrolytic graphite (HOPG) surface. Images of the surface are used to determine the crystal structure of the material, and scanning tunneling spectroscopy is used to determine the electronic properties of the material and study the tunneling phenomenon. In the second experiment, the students image the Au(111) surface as well as a series of alkanethiol self-assembled monolayers (SAMs) of different chains lengths on the Au(111) surface. They examine the structural and electronic properties of the metal surface and the adlattice structure of the film. Finally, in the third experiment, the students examine the conductance of molecules adsorbed onto the Au(111) surface, including the alkanethiol SAMs and a thiol-tethered porphyrin molecule or a dimercaptostilbene embedded into the SAM matrix. By measuring the tunneling efficiency and spectroscopic characteristics of these molecules, the students can explore the relationship between chemical structure and charge transport efficiency. The experiments provide advanced chemistry students an opportunity to view and study materials at the atomic and molecular length scales and provide an opportunity to apply their understanding of quantum mechanical concepts to real systems.

KEYWORDS: Upper-Division Undergraduate, Laboratory Instruction, Physical Chemistry, Hands-On Learning/Manipulatives, Nanotechnology, Physical Properties, Spectroscopy, Surface Science



Scanning probe techniques, including scanning tunneling microscopy (STM), atomic force microscopy (AFM), and the many derivatives of these techniques, are gaining considerable traction in chemical and biological investigations and the field of materials science and engineering in general.¹ Familiarity with these techniques will help undergraduate students explore how modern physical chemistry and analytical methods are applied in research. We have developed a physical chemistry laboratory with this in mind, focused on demonstrating cutting edge techniques and instrumentation used by chemists, including in particular STM. Not only does this offer students exposure to such relevant techniques, it also reinforces their understanding of quantum mechanics and the chemical structure of solids. Several experiments have been reported that introduce students to the STM in the teaching laboratory, each with its own unique focus and goals including the study of surface structure,² adsorbate structure and intermolecular interactions,^{3,4} nanomaterials,⁵ and reaction kinetics.⁶ This experiment introduces a similar series of topics, though with considerable emphasis on the mechanisms and quantum mechanical process of tunneling as well as the relationship between molecular structure and electron transport. The topics considered in this series include the basics of electron tunneling

and the quantum mechanical description of this phenomenon; the structure of crystals, surfaces, and adlayers; solid-state properties of materials; and investigation of charge transfer mechanisms through molecules using scanning tunneling spectroscopy (STS), the latter being relevant to a range of subjects including biological systems, the development of photovoltaic and other molecular or organic electronics applications and incorporating discussions of the relationships between chemical and electronic structure of complex molecules.

The experiments described herein are part of a physical chemistry laboratory in the first semester of a two-semester sequence (1 credit each) focusing on the theme of quantum mechanics, which parallels the physical chemistry lecture sequence that covers quantum mechanics in the first semester and thermodynamics in the second semester. Students are required to complete the prerequisite lecture in advance of taking the lab. The laboratories are taken by a mix of third-year (~20%) and fourth-year (~80%) students. This experiment is conducted over a three-week span and is broken into three

Published: January 8, 2014

distinct parts. The first week is reminiscent of many prior studies,^{3,4,7} introducing the fundamentals of STM. The students begin by characterizing highly oriented pyrolytic graphite (HOPG), as this surface is easily prepared and atomic resolution of the surface is achieved with minimal effort. Here, the students learn about the structure of solids and surfaces and begin their investigation into the electron tunneling process with spectroscopic measurements while familiarizing themselves with the instrumentation and imaging process. In the second week, the students examine the surface of gold, with and without alkanethiol self-assembled monolayers (SAMs). In addition to reinforcing topics discussed in the first experiment, this section introduces the concept of surface adsorbates and their adlattice structure and presents the notion of electron tunneling through different mediums. Finally, in the third week, the students examine charge transport through a thiol-tethered porphyrin molecule, wherein they are encouraged to consider the structure of the molecule and measurements made both by imaging and spectroscopy, as well as consultation with the literature, to determine the mechanism of electron transport through the molecule. Each experiment is designed to be wholly conducted within 3 h, including sample preparation, instrument setup, and clean up, the vast majority of which is conducted by the students under the guidance of an instructor. Although the molecule we have used is unique to our physical chemistry lab, we also demonstrate here the use of a 4,4'-dimercaptostilbene that is commercially available.

EQUIPMENT AND MATERIALS

A Nanosurf Easyscan2 STM (Nanosurf; Liestal, Switzerland) with a 500 nm low current scanner was used. Pt/Ir tip wire (Nanoscience Instruments, Phoenix, AZ, 0.25 mm diameter) was used, using mechanical cleaving performed initially by the instructor for demonstration but ultimately by the students themselves. HOPG (Nanoscience Instruments) was cleaved prior to imaging with scotch tape to present a clean surface. Flame-annealed Au on mica substrates obtained from Agilent Technologies (Phoenix, AZ) and Phasis (Geneva, Switzerland) were cleaned by UV-ozone exposure immediately prior to use. Molecules used included decanethiol, dodecanethiol, octadecanethiol, and 4,4'-dimercaptostilbene and were obtained from Sigma Chemicals and used as received. For studies of molecular conductance, a tailor-made thiol-tethered freebase porphyrin was used, and its synthesis and conductance properties have been previously described.⁸ This experiment was also demonstrated with the dimercaptostilbene molecule. Image analysis was performed using the freely available Gwyddion software package.⁹ Complete details of the instrumentation, methods, and implementation of these instructional experiments may be found in the Supporting Information.

HAZARDS

Gloves and goggles should be worn during all sample and solution preparation as well as during handling of the samples and the scanning tunneling microscope. Decanethiol, dodecanethiol, and octadecanethiol are irritants, and these along with 4,4'-dimercaptostilbene are highly toxic if consumed. Tetrahydrofuran (THF) and ethanol are flammable. All solvents and chemicals should be used in a chemical hood to minimize exposure.

EXPERIMENTAL DETAILS

Week 1: The Structure and Electronic Properties of Highly Oriented Pyrolytic Graphite (HOPG)

Many previous reports have been made using HOPG to illustrate the capabilities of STM and introduce students to the examination of atomic structure,^{3,4,7} and this part of the experiment is similar. An image of the HOPG surface collected by a student group is shown in Figure 1 along with a Fourier-

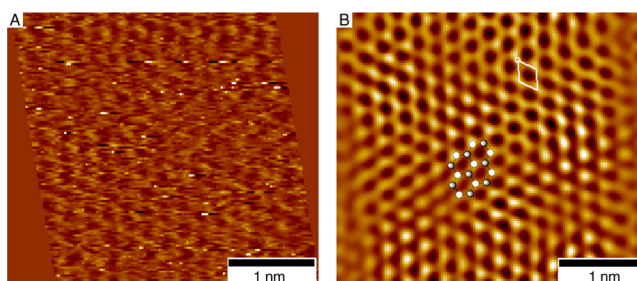


Figure 1. (A) Student-collected image of the graphite surface. Though noisy, applying a Fourier filter (B) provides the students with a clearer image as well as provides a review and demonstrates an application of this noise-reduction technique. These images have been drift-corrected based on the known lattice of HOPG. Bias 40 mV; set point 1.4 nA.

transformed image that clearly shows the lattice structure of the graphite surface. We find that guiding the students through this filtering process introduces students to concepts of data and image processing and visually illustrates this important noise-reduction technique. The students are instructed to use the images to reconstruct the crystalline lattice from the measured dimensions of the surface lattice and interlayer spacing, familiarizing themselves with the concepts of a crystal lattice and how STM can be used to deduce the crystal lattice based on surface measurements. Additionally, the HOPG surface conveniently illustrates that STM is not sensitive to nuclear positions but rather to electronic state density, giving rise to the contrast observed between the two unique atoms in the surface unit cell.

The relevant quantum mechanical concepts are also first introduced in this experiment. The students collect both $I-z$ (current vs tip position) and $I-V$ (current vs voltage) spectra. From the former, they can determine the quantum mechanical potential barrier height, and from the latter they can investigate the density of states of the graphite material. As graphite is a semimetal, the junction follows Ohm's law, and they simply obtain a linear relationship between current and bias, shown in Figure 2A, which is compared to a Au surface (Figure 2B) in week 2. The slight deviation to lower conductivity near zero bias reflects the semimetal nature of the HOPG, wherein a momentum shift between the valence and conduction bands gives rise to reduced conductivity at low bias. Figure 3A illustrates the determination of the barrier height using the formula¹⁰

$$\ln(I) = -A\sqrt{\phi}z + C = -\beta z + C \quad (1)$$

The independent variable z reflects the gap width. In scanning tunneling spectroscopy (STS), the gap width is not known and all values are referenced to the position of the tip dictated by the feedback loop. The offset between the actual gap width and reported tip position, among other factors including bias and conductivity of the gap, is captured in the

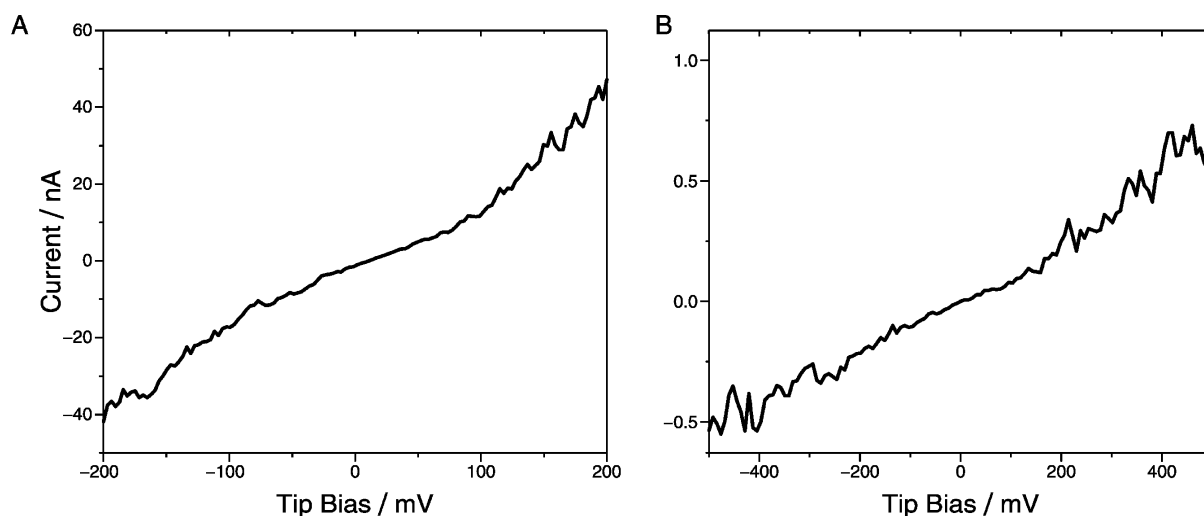


Figure 2. I - V spectra of HOPG (A) and Au(111) (B) demonstrating the metallic character of these two materials. Because these materials are metallic, Ohm's law applies and a linear relation between current and bias is observed. The slight suppression of conductivity near 0 V in (A) is indicative of the semimetallic electronic structure of HOPG.

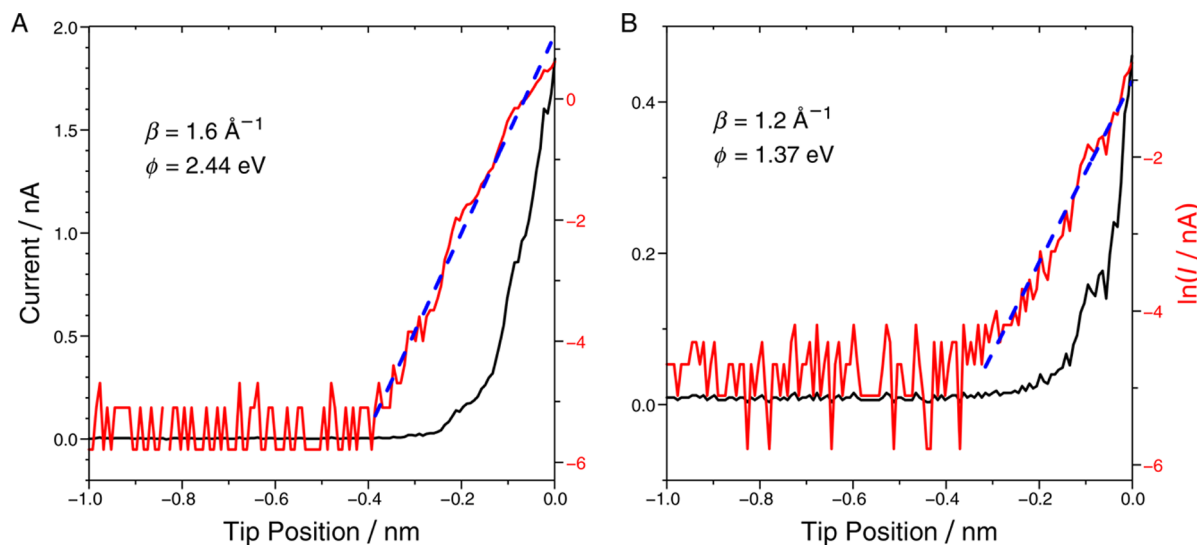


Figure 3. I - z spectra collected on the HOPG (A) and Au(111) (B) surface showing the I - z spectrum (black), with corresponding semilog plot (red) shown. The tunneling efficiency can be determined by a linear fit (blue), producing the tunneling efficiencies (β) and barrier heights (ϕ) shown. The difference in barrier height reflects the different Fermi levels of the two substrates and the different biases applied during imaging.

arbitrary constant C . The value A is a constant with value 1.025 \AA^{-1} when ϕ , the quantum mechanical potential barrier height, is given in eV.¹¹ The more general parameter, β , termed the tunneling efficiency, can similarly be determined from the I - z spectrum as described in eq 1. This value reflects the rate of decay of the wave function in the tunneling region. Again, this is compared to Au (Figure 3B) in week 2.

Week 2: Au(111) and Self-Assembled Monolayers (SAMs) on Au(111)

In week 2, the students focus their interest on adsorbed layers on a metal surface. The students are first asked to image a bare gold surface. In doing so, the substrate is introduced, and topics including the structure of metal crystals (fcc, bcc, and hcp) along with how different crystal faces (defined by their Miller indices) are projected as surface structures can be discussed. The basic features of the gold surface are examined, including the interlayer spacing of the Au(111) planes. The students are encouraged to briefly attempt to resolve the atomic structure of

the surface; however, under ambient conditions, success is highly unlikely. This, however, serves to further illustrate the role of the electronic structure in imaging and encourages the students to consider the differences in the electronic structures of graphite and Au(111), where the more localized valence orbitals of graphite provide greater contrast and greater effective signal

An example of a student group's determination of the interlayer spacing is presented in Figure 4. The students also perform spectroscopy on this surface, generating both I - V and I - z spectra (Figure 2B and Figure 3B, respectively). To reinforce the connection between the quantum mechanical aspect of tunneling and the configuration of the experiment, the students are directed to compare the tunneling efficiency and barrier height between this surface and graphite. Differences in these measurements reflect the different imaging biases employed and the different work function of the materials, which together lead to changes in the effective barrier height.

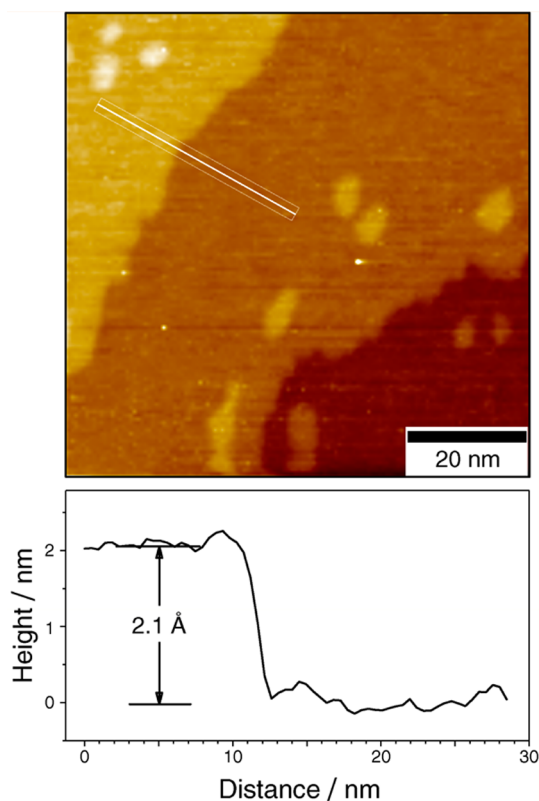


Figure 4. Bare gold surface imaged under ambient conditions showing the interlayer spacing of the Au(111) atomic layers. The students measured 2.1 Å here, reasonably close to the expected value of 2.3 Å. The marks on this surface are likely contamination, as the sample is handled and imaged under ambient conditions. Bias 0.5 V; set point 0.5 nA.

The students are also asked to determine the source of and magnitude of the resistance in the tunnel junctions to connect the involved quantum mechanics to more traditional concepts of electronic circuitry.

Imaging of the gold surface and discussion of its properties precedes the discussion and imaging of the alkanethiol self-assembled monolayers so that the students may better understand the substrate before considering the adsorbed layer. Alkanethiol SAMs have been extensively studied^{13–15} and, therefore, make an ideal system for the students to both investigate in the lab and in the literature. The students prepare

their self-assembled monolayers, cleaning the gold surface and preparing the immersion solutions (0.1–1.0 mM in ethanol), learning basic concepts about surface preparation and properties. During imaging, they are encouraged to examine all aspects of the surfaces at various length scales. At larger scales, they observe a surface that effectively appears identical to the gold surface (Figure 5A). As they observe the surface on smaller length scales, they will observe the typical etch pits found on the alkanethiol functionalized Au(111) surface (Figure 5B). Here, the students are encouraged to review the literature to consider the proposed mechanisms of SAM formation. A variety of references are available from which the students could generate a rational hypothesis.^{16,17} Finally, the students can observe various adlattices of the alkanethiols. This is a very difficult image to collect and extract measurements of the adlattice, so we supplement this experiment by directing the students to the literature to obtain an understanding of the adlattice structure as well as providing sample images. A student-collected image is shown in Figure 5C. It should be noted that a very stable tip and stable imaging conditions are required for successful imaging with molecular resolution.

Determining the tip position relative to the SAM is a challenging task but is one which $I-z$ spectroscopy can be used to determine.¹³ Furthermore, changes to the tunnel barrier with addition of the monolayer can be characterized by measuring the tunneling rate decay. An $I-z$ spectrum of a decanethiol SAM is shown in Figure 6A, with the corresponding semilog plot in Figure 6B. The most important feature here is the change in decay rate as the tip descends. The two tunneling regimes correspond to the tip above and within the monolayer, demonstrating that the tip resides just a few angstroms above the decanethiol SAM surface.

To challenge the student's critical thinking and improve their understanding of the technique and the role of the feedback loop in dictating the tip position, the students are also asked to replicate a measurement in which the conductivity of the alkanethiols are compared as a function of length.¹⁸ Figure 7A shows $I-V$ spectra of the three alkanethiol monolayers studied, and 7B shows a semilog plot of the conductance, measured at 1 V, from these spectra plotted against the thickness of the films. The basis for this type of measurement is an AFM study of molecular conductance, in which the conductivity of films is measured as a function of film thickness. However, where in AFM the tip position is dictated by the film thickness, in STM, the feedback loop and set point current dictate the tip position. This is most critical for the octadecanethiol data point in Figure

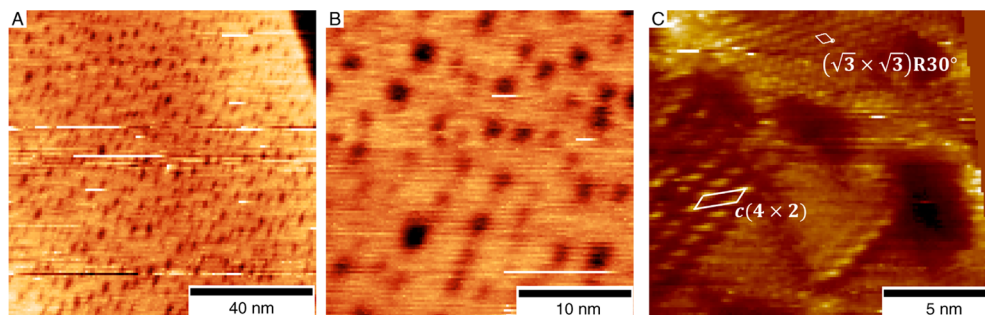


Figure 5. Images at various scales of decanethiol on Au(111). It is possible to see the broader structures of the gold surface (A) and the SAM (B) as well as the molecular structures of the monolayer (C), where both the typical $(\sqrt{3} \times \sqrt{3})R30^\circ$ structure as well as the more compressed $c(4 \times 2)$ structure¹² are visible. Note: Image (C) is an image of the current flow as a function of position that has also been corrected for drift, using the $(\sqrt{3} \times \sqrt{3})R30^\circ$ alkanethiol lattice structure as a reference. (A, B) 1.4 V; 75 pA. (C) 1.4 V; 100 pA.

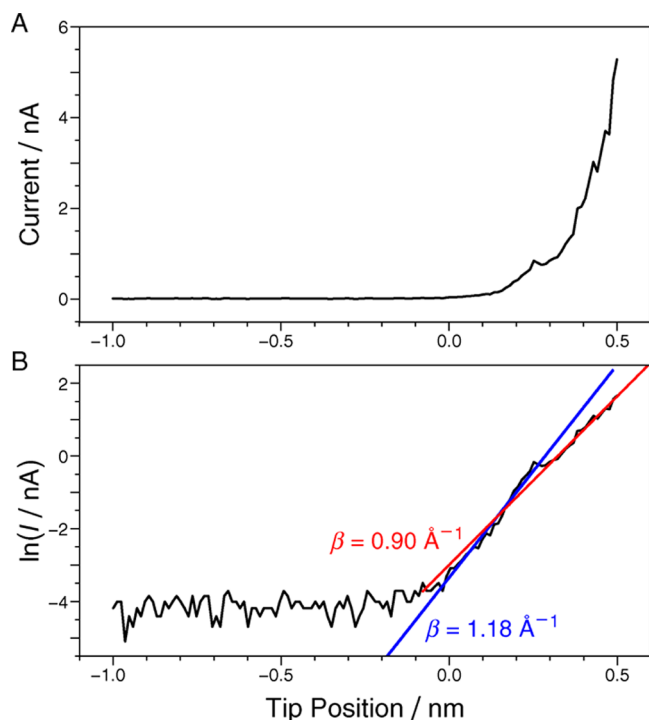


Figure 6. I - z spectroscopy of the decanethiol film (A) and the corresponding semilog plot (B). A modest change in tunneling efficiency is observed in the spectrum, corresponding to the transition from the tip being above the monolayer (blue trend line) and within the monolayer (red trend line), as has been previously observed.¹³

7B. This film is too thick for the tip to be positioned above the film at any measurable tunnel current; therefore, the feedback loop positions the tip within the film. This results in a greater conductance measurement, producing a very high, but erroneous, tunneling efficiency.

Week 3: Molecular Charge Transport

The last set of experiments is designed to demonstrate the STM's ability to measure the electronic properties of individual molecules, demonstrating a chemist's ability to examine charge transport in single molecules directly. A variety of methods have been developed to study molecular charge transport,^{19,20} and considerable work has been conducted examining the effects of chemical²¹ and conformational structure.²² The greatest challenge of studying single-molecule electron transport is adequately controlling the geometry and environment of the molecule. Forming SAMs of the molecule of interest²³ or embedding the molecule in SAM support matrix^{8,24} have been used successfully. The first experiment reported here was performed on a tailor-made molecule; however, at the end of this section, a commercially available alternative is also presented. Here, a SAM of dodecanethiol is used to control the orientation of the molecule and to act as a reference for studying its electronic properties. The students prepare a mixed monolayer of porphyrin with a thiol tether in a dodecanethiol matrix⁸ (this is depicted in Figure 8C), and they image it in much the same manner as the alkanethiol SAMs. They are instructed to collect the I - V spectra of the porphyrins as well as images from which the apparent height of the porphyrins can be determined. The I - V spectra are collected on the background monolayer as well, for use as a comparison. From the I - V spectra, they can begin to make assumptions about the charge transport characteristics. For example, for the

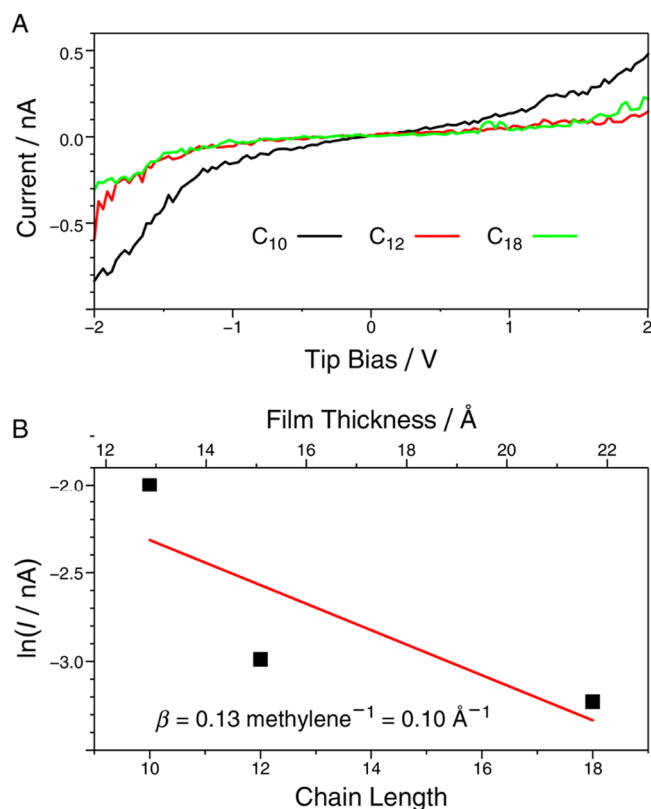


Figure 7. (A) I - V spectra of decanethiol, dodecanethiol, and octadecanethiol demonstrating the progressive decrease in current flow, particularly at higher bias, indicative of greater tip sample separation. (B) The log of the current measured at 1.0 V from the I - V spectra plotted as a function of film thickness, producing an erroneously high tunneling efficiency because the tip position is not directly related to the film thickness.

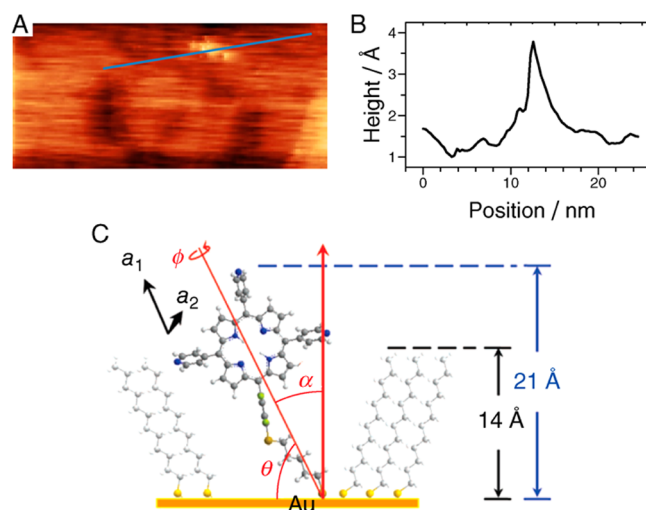


Figure 8. STM topographic image of the porphyrin molecule embedded in the dodecanethiol matrix (A) and the corresponding cross section demonstrating an approximate apparent height of 3 Å (B). This apparent height may be used in conjunction with the known physical height of 7 Å, shown in (C), to determine the average tunneling efficiency of the molecule by the double-layer tunnel junction model, resulting in an average tunneling efficiency of 1.2 \AA^{-1} , quite similar to that of an alkanethiol.

thiol-tethered porphyrin, they most often measure approximately higher current magnitude, with similar spectrum shape, shown in Figure 9. The greater current at higher bias suggests

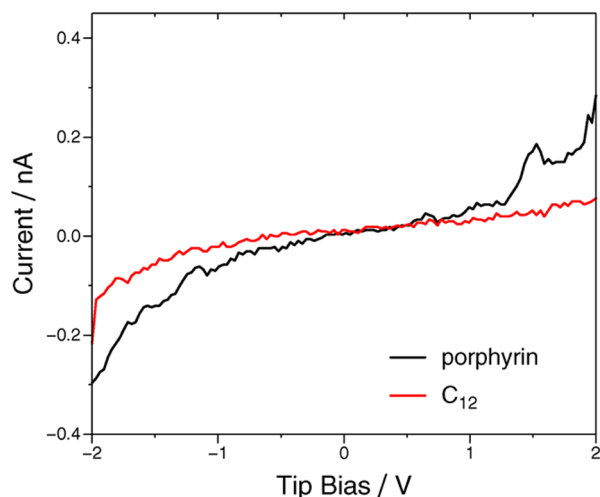


Figure 9. I - V spectra of the thiol-tethered porphyrin (black) superimposed over the spectrum of dodecanethiol (red), showing higher, but not dramatically higher, current magnitude and similar spectrum shape, indicating dominance of the alkyl chain tether in the electron tunneling process.

that the porphyrin is more conductive at higher bias, but the similar spectral shape would suggest that the alkyl tether is the dominant structural feature in the conductance of this molecule.

The last measurement the students are instructed to make is a measurement of the tunneling efficiency of the porphyrin using the double-layer tunnel junction model.²⁵ This method provides a measure of the tunneling efficiency of the molecule as a whole and demonstrates the dominant transport mechanism present in the molecule. From this model, the tunneling efficiency of the molecule may be determined by using the apparent height measured from STM imaging. The following equation may be used to determine the tunneling efficiency, β

$$\beta = [\beta_{\text{DDT}}h_{\text{DDT}} - \alpha(\delta h_{\text{STM}} - \delta h)]/h_{\text{pn}} \quad (2)$$

The dodecanethiol matrix acts as an internal standard, with its tunneling efficiency, β_{DDT} , and thickness, h_{DDT} , known (1.2 \AA^{-1} and 14 \AA , respectively). A vacuum gap is assumed above both the monolayer and the porphyrin, with tunneling efficiency α (2.3 \AA^{-1}). The tunneling efficiency is ultimately reflected in the difference between the actual protrusion height, δh , and the apparent height measured by STM, δh_{STM} . The students are guided through the determination of h_{pn} , the total height of the porphyrin molecule based on its known orientation and length, from which δh can be determined by deducting the thickness of the film. The total height and physical protrusion height are 21 \AA and 7 \AA , respectively. From the measured apparent height, a tunneling efficiency of 1.2 \AA^{-1} is obtained from the data shown here, in agreement with the reported value in the literature.⁸ For this molecule, a tunneling efficiency very similar to that of alkanethiols is observed,⁸ further indicating that the tether is the dominant part of the charge transport process. Because prior characterization is necessary for the students to validate their results, the choice of

molecules is generally limited to those already examined in the literature.^{25,26} One could envision, however, using this lab as a way of exploring additional unknown molecules for comparison to known systems.

The charge transport characteristics are related to the electronic structure of the molecule; therefore, to assist the students in rationalizing the charge transport properties of the porphyrins, it is necessary to discuss the electronic structure of the porphyrin. Understanding the relationship between chemical structure, electronic structure, and charge transport characteristics is a relatively new area of research; however, there are some general themes that are within the grasp of a new chemist. Most important to molecular electron transport is the energy of the frontier orbitals and their localization on the molecule. In the case shown here, the HOMO and LUMO are localized to the porphyrin macrocycle itself, and they are roughly 2-fold degenerate. The HOMO-LUMO gap has been determined to be approximately 1.8 eV, determined by DFT calculations, with the HOMO calculated to be displaced from the Au Fermi level by only 0.2 eV.⁸ Although this latter point may not be particularly accurate due to the inaccuracy of absolute energies by computation methods, at a bias of $\pm 2.0 \text{ V}$, it is likely that one or both frontier orbitals is within the bias window and, therefore, resonant tunneling through the porphyrin ring should be possible. As is shown here, the tunneling efficiency of this thiol-tethered porphyrin is comparable to the alkanethiol matrix, suggesting that tunneling is dominated by the alkanethiol tether under the imaging conditions employed. This could be explained due to the fact that the frontier orbitals are decoupled from the substrate by the alkanethiol tether, or they may not be present in the bias window at the imaging bias of 1.4 V. Because this research is generally performed using statistical analysis of a large number of results over several samples and with several tips, it is not unlikely that the students will obtain results that vary; as such, we attempt to arm them with sufficient information that they can use to rationalize their individual results as well as providing them with sample data sets in case the results are too incoherent for a reasonable analysis.

To facilitate the broad dissemination of this experiment, an alternative, commercially available molecule, 4,4'-dimercaptostilbene, has also been examined. This molecule has been previously characterized²⁵ and behaves quite similarly to the porphyrin thiol molecule for the purposes of this experiment. An STM topographic image of the mixed monolayer is shown in Figure 10 with the corresponding insertion geometry. From the image shown, the apparent height was measured to be $4.0 \text{ \AA} \pm 0.2 \text{ \AA}$, in perfect agreement with value reported in the literature.²⁵ The tilt of the molecule has not been directly characterized, as it does not protrude from the monolayer, but it is presumed to insert perpendicular to the surface, such that its physical height is 13.9 \AA , yielding a tunneling efficiency of 0.6 \AA^{-1} . The significantly higher tunneling efficiency of this molecule can be attributed to its entirely conjugated structure, which yields a small HOMO-LUMO gap and facilitates electron transmission through the entire molecule. Investigating a series of molecules with different dimensions and chemical connectivity allows for students to develop an appreciation for the interplay between the physical dimensions of a molecule and its electronic properties and how their properties combine to produce the observed apparent height of a molecule in an STM image.

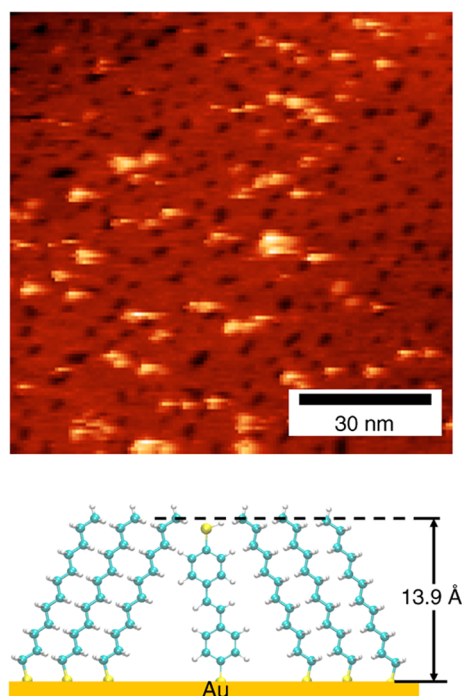


Figure 10. Topography of 4,4'-dimecaptostilbene, dodecanethiol mixed SAM (1.4 V; 70 pA). The protrusions correspond to stilbene molecules, with an apparent height of 4.0 ± 0.2 Å. The insertion geometry of the molecules is shown below the topography figure.

CONCLUSION

This series of experiments has proven both engaging and challenging for the students in our physical chemistry laboratory. They are often intrigued by the notion that, in a relatively simple laboratory setting, it is possible to observe atomic and molecular structure. With this ability, they are able to develop and apply their understanding of crystal and surface structures to systems that they can directly measure. Additionally, it allows them to apply the techniques and concepts learned in their concurrent physical chemistry lecture courses, aiding in internalizing the concepts of electron wave functions and tunneling behavior. In these areas, the students are quite successful. Developing a working understanding of molecular electronic structure and applying it to the concept of molecular conductance is the most challenging aspect of this series of experiments for the students. However, because the experiments are conducted in a small-group setting under the guidance of a skilled instructor, the majority of students are capable of internalizing these concepts and applying them in this setting.

ASSOCIATED CONTENT

Supporting Information

A copy of the student handbook that we include with this experiment is provided in the Supporting Information, as well as experimental procedures and sample questions. Information for instructors including instrumentation, imaging, and preparation details are also included. This material is available via the Internet at <http://pubs.acs.org>.

AUTHOR INFORMATION

Corresponding Author

*J. D. Batteas. E-mail: batteas@chem.tamu.edu.

Present Address

[§]Intel Corporation, 5000 W. Chandler Blvd. Chandler, Arizona 85226, United States

Notes

The authors declare no competing financial interest.

ACKNOWLEDGMENTS

We gratefully acknowledge the support of this work and the associated lab development from the National Science Foundation (CHE-0848786 and CHE-1213802) and the Department of Chemistry and The Association of Former Students of Texas A&M University. We would also like to acknowledge the input and improvements in these experiments over the past few years by Dr. Ryan Jones (now at Total Petrochemical, Houston, TX) and Professors Simon North and Dong Hee Son, Department of Chemistry, Texas A&M University. We also wish to thank Professor Charles M. Drain, Hunter College of CUNY for providing the porphyrin thiol derivative used in this study.

REFERENCES

- (1) Roa, J. J.; Oncins, G.; Díaz, J.; Capdevila, X. G.; Sanz, F.; Segarra, M. Study of the friction, adhesion and mechanical properties of single crystals, ceramics and ceramic coatings by AFM. *J. Eur. Ceram. Soc.* **2011**, *31*, 429–449.
- (2) Braun, R. D. Scanning tunneling microscopy of silicon and carbon. *J. Chem. Educ.* **1992**, *69*, A90.
- (3) Giancarlo, L. C.; Fang, H.; Avila, L.; Fine, L. W.; Flynn, G. W. Molecular Photography in the Undergraduate Laboratory: Identification of Functional Groups Using Scanning Tunneling Microscopy. *J. Chem. Educ.* **2000**, *77*, 66.
- (4) Pullman, D.; Peterson, K. I. Investigating Intermolecular Interactions via Scanning Tunneling Microscopy. An Experiment for the Physical Chemistry Laboratory. *J. Chem. Educ.* **2004**, *81*, 549.
- (5) Furlan, P. Y. Engaging Students in Early Exploration of Nanoscience Topics Using Hands-On Activities and Scanning Tunneling Microscopy. *J. Chem. Educ.* **2009**, *86*, 705.
- (6) Poler, J. C. Surface Oxidation Kinetics: A Scanning Tunneling Microscopy Experiment. *J. Chem. Educ.* **2000**, *77*, 1198.
- (7) Zhong, C.-J.; Han, L.; Maye, M. M.; Luo, J.; Kariuki, N. N.; Jones, W. E. Atomic Scale Imaging: A Hands-On Scanning Probe Microscopy Laboratory for Undergraduates. *J. Chem. Educ.* **2003**, *80*, 194.
- (8) Chan, Y.-H.; Schuckman, A. E.; Perez, L. M.; Vinodu, M.; Drain, C. M.; Batteas, J. D. Synthesis and Characterization of a Thiol-Tethered Tripyridyl Porphyrin on Au(111). *J. Phys. Chem. C* **2008**, *112*, 6110–6118.
- (9) Gwyddion. <http://www.gwyddion.net> (Accessed Dec 2013).
- (10) Olesen, L.; Brandbyge, M.; Sørensen, M. R.; Jacobsen, K. W.; Lægsgaard, E.; Stensgaard, I.; Besenbacher, F. Apparent Barrier Height in Scanning Tunneling Microscopy Revisited. *Phys. Rev. Lett.* **1996**, *76*, 1485–1488.
- (11) Hansma, P. K.; Tersoff, J. Scanning tunneling microscopy. *J. Appl. Phys.* **1987**, *61*, R1–R24.
- (12) Poirier, G. E.; Tarlov, M. J. The $c(4 \times 2)$ Superlattice of n-Alkanethiol Monolayers Self-Assembled on Au(111). *Langmuir* **1994**, *10*, 2853–2856.
- (13) Yang, G.; Liu, G.-y. New Insights for Self-Assembled Monolayers of Organothiols on Au(111) Revealed by Scanning Tunneling Microscopy. *J. Phys. Chem. B* **2003**, *107*, 8746–8759.
- (14) Picraux, L. B.; Zangmeister, C. D.; Batteas, J. D. Preparation and Structure of a Low-Density, Flat-Lying Decanethiol Monolayer from the Densely Packed, Upright Monolayer on Gold. *Langmuir* **2005**, *22*, 174–180.
- (15) Poirier, G. E. Characterization of Organosulfur Molecular Monolayers on Au(111) using Scanning Tunneling Microscopy. *Chem. Rev.* **1997**, *97*, 1117–1128.

(16) Poirier, G. E. Mechanism of Formation of Au Vacancy Islands in Alkanethiol Monolayers on Au(111). *Langmuir* **1997**, *13*, 2019–2026.

(17) Torres, E.; Blumenau, A. T.; Biedermann, P. U. Mechanism for phase transitions and vacancy island formation in alkylthiol/Au(111) self-assembled monolayers based on adatom and vacancy-induced reconstructions. *Phys. Rev. B* **2009**, *79*, 075440.

(18) Monnell, J. D.; Stapleton, J. J.; Dirk, S. M.; Reinerth, W. A.; Tour, J. M.; Allara, D. L.; Weiss, P. S. Relative Conductances of Alkaneselenolate and Alkanethiolate Monolayers on Au{111}. *J. Phys. Chem. B* **2005**, *109*, 20343–20349.

(19) Chen, F.; Hihath, J.; Huang, Z.; Li, X.; Tao, N. J. Measurement of Single-Molecule Conductance. *Annu. Rev. Phys. Chem.* **2007**, *58*, 535–564.

(20) Gonzalez, C.; Simón-Manso, Y.; Batteas, J.; Marquez, M.; Ratner, M.; Mujica, V. A Quasimolecular Approach to the Conductance of Molecule–Metal Junctions: Theory and Application to Voltage-Induced Conductance Switching. *J. Phys. Chem. B* **2004**, *108*, 18414–18420.

(21) Chen, F.; Li, X.; Hihath, J.; Huang, Z.; Tao, N. Effect of Anchoring Groups on Single-Molecule Conductance: Comparative Study of Thiol-, Amine-, and Carboxylic-Acid-Terminated Molecules. *J. Am. Chem. Soc.* **2006**, *128*, 15874–15881.

(22) Venkataraman, L.; Klare, J. E.; Nuckolls, C.; Hybertsen, M. S.; Steigerwald, M. L. Dependence of single-molecule junction conductance on molecular conformation. *Nature* **2006**, *442*, 904–907.

(23) Hacker, C. A.; Batteas, J. D.; Garno, J. C.; Marquez, M.; Richter, C. A.; Richter, L. J.; van Zee, R. D.; Zangmeister, C. D. Structural and Chemical Characterization of Monofluoro-Substituted Oligo-(phenylene–ethynylene) Thiolate Self-Assembled Monolayers on Gold. *Langmuir* **2004**, *20*, 6195–6205.

(24) Dunbar, T. D.; Cygan, M. T.; Bumm, L. A.; McCarty, G. S.; Burgin, T. P.; Reinerth, W. A.; Jones, L.; Jackiw, J. J.; Tour, J. M.; Weiss, P. S.; et al. Combined Scanning Tunneling Microscopy and Infrared Spectroscopic Characterization of Mixed Surface Assemblies of Linear Conjugated Guest Molecules in Host Alkanethiolate Monolayers on Gold. *J. Phys. Chem. B* **2000**, *104*, 4880–4893.

(25) Moth-Poulsen, K.; Patrone, L.; Stuhr-Hansen, N.; Christensen, J. B.; Bourgoin, J.-P.; Bjørnholm, T. Probing the Effects of Conjugation Path on the Electronic Transmission through Single Molecules Using Scanning Tunneling Microscopy. *Nano Lett.* **2005**, *5*, 783–785.

(26) Tour, J. M.; Rawlett, A. M.; Kozaki, M.; Yao, Y.; Jagessar, R. C.; Dirk, S. M.; Price, D. W.; Reed, M. A.; Zhou, C.-W.; Chen, J.; et al. Synthesis and Preliminary Testing of Molecular Wires and Devices. *Chem.—Eur. J.* **2001**, *7*, 5118–5134.